

# Recurrence plots and Shannon entropy for a dynamical analysis of asynchronisms in noninvasive mechanical ventilation

H. Rabarimanantsoa

*CORIA UMR 6614, Université de Rouen, Av. de l'Université, BP 12, F-76801 Saint-Etienne du Rouvray Cedex, France*

L. Achour<sup>a)</sup>

*ADIR Association, Hôpital de Bois-Guillaume, 147, av. du Maréchal, 76031 Rouen Cedex, France*

C. Letellier

*CORIA UMR 6614, Université de Rouen, Av. de l'Université, BP 12, F-76801 Saint-Etienne du Rouvray Cedex, France*

A. Cuvelier<sup>a)</sup> and J.-F. Muir<sup>a)</sup>

*Service de Pneumologie et Soins Intensifs, Hôpital de Bois-Guillaume, Centre Hospitalier Universitaire de Rouen, 76031 Rouen Cedex, France*

(Received 3 May 2006; accepted 1 January 2007; published online 21 March 2007)

Recurrence plots were introduced to quantify the recurrence properties of chaotic dynamics. Hereafter, the recurrence quantification analysis was introduced to transform graphical interpretations into statistical analysis. In this spirit, a new definition for the Shannon entropy was recently introduced in order to have a measure correlated with the largest Lyapunov exponent. Recurrence plots and this Shannon entropy are thus used for the analysis of the dynamics underlying patient assisted with a mechanical noninvasive ventilation. The quality of the assistance strongly depends on the quality of the interactions between the patient and his ventilator which are crucial for tolerance and acceptability. Recurrence plots provide a global view of these interactions and the Shannon entropy is shown to be a measure of the rate of asynchronisms as well as the breathing rhythm. © 2007 American Institute of Physics. [DOI: 10.1063/1.2435307]

**When spontaneous breathing is no longer sufficient to maintain alveolar ventilation and subsequent gas exchange, noninvasive mechanical ventilation that allows a reduction in the work of breathing is an effective procedure to relieve the patients with chronic respiratory diseases. One important dynamical feature involved in the patient discomfort is the lack of synchronization between the patient's breathing rhythm and the ventilator cycle. The dynamics underlying the patient-ventilator interactions is thus investigated using recurrence plots and the Shannon entropies which can be estimated from them. The Shannon entropies computed from the airway pressure and from the total duration of the respiratory cycle provide a classification of the types of patient-ventilator interactions observed. They could be used to quickly set the ventilator.**

## I. INTRODUCTION

Noninvasive mechanical ventilation is an effective procedure to manage patients with acute or chronic respiratory failure. Most ventilators act as flow generators that assist spontaneous respiratory cycles by delivering inspiratory and expiratory pressures. Alveolar ventilation and subsequent pulmonary gas exchanges are thus improved. Since the system patient-ventilator can be viewed as a nonlinear dynamical

system, the application of the nonlinear dynamical system theory to the analysis of the respiratory rhythm during mechanical ventilation can be traced back to the analysis of different coupling patterns (between a mechanical ventilator and the respiratory rhythm) in the works by Petrillo and Glass<sup>1,2</sup> where the concept of phase locking was first proposed. Experiments were performed on anesthetized cats which were paralyzed by neuromuscular blockade and invasively ventilated. The rhythm of central respiratory activity was monitored by recording inspiratory-promoting activity from the phrenic nerve that innervates the diaphragm. As the ventilator volume and frequency varied, a number of different rhythms were identified between the ventilator and phrenic activity.<sup>2</sup>

Tools borrowed from nonlinear dynamical systems theory have been widely used in biomedicine, in particular for investigating cardiac variability, see Refs. 3–6, among others. Breathing is a phenomenon naturally related to the cardiac activity as shown by the global model obtained by Aguirre and co-workers.<sup>7</sup> Also in normal subjects, breathing patterns display a certain variability which is maintained by a central neural mechanism and the feedback loop of arterial chemoreceptors and lung vagal sensory receptors.<sup>8</sup> Peripheral factors, such as mechanical and chemical changes within the respiratory system, may modify the breathing pattern variability from the normal level in individuals with pathological conditions. Quantitative methods, including calculations of coefficients of variations and first-return maps—also

<sup>a)</sup>Also at UPRES EA 3830—IFR MP23, Université de Rouen, France.

called Poincaré maps—have been applied to the analysis of breathing pattern variability to serve as indicators of pathological conditions in patients with respiratory diseases.<sup>9–11</sup>

One of the relevant factors for the tolerance of the assisted mechanical ventilation could be related to the patient comfort. Unfortunately, quantifying ventilatory comfort is still an open problem since it is based on subjective answers to questions asked to the patient. Our objective is therefore to investigate how tools borrowed from the nonlinear dynamical systems theory can improve this subjective estimation of the patients' comfort. This will be done by assuming that two particular factors could play an important role in the tolerance of mechanical ventilation. They are asynchronisms—generally, an asynchronism corresponds to a lack of ventilator triggering by inspiratory effort of the patient—and the regularity of the breathing rhythm. It will be shown that both can be related with some recurrence properties of the dynamics.

In order to investigate these properties the recurrence plots introduced by Eckmann, Kamphorst, and Ruelle<sup>13</sup> will be used. A *recurrence plot*  $R_{ij}$  is a square array built as follows. Every point of the phase space trajectory  $\{\mathbf{x}_{ij}\}_{i=1}^N$  is tested whether it is close to another point  $\mathbf{x}_j$  of the trajectory, that is, whether the distance between these two points is less than a specified threshold  $\epsilon$ . In this case, the point is said to be recurrent and is represented by a black dot. Otherwise, the point is not recurrent and is represented by a white dot. This can be described as an  $N \times N$  array

$$R_{ij} = \theta(\epsilon - \|\mathbf{x}_i - \mathbf{x}_j\|), \quad (1)$$

where  $\theta(\mathbf{x}_i)$  is the Heaviside function.

A few years later, Trulla *et al.*<sup>14</sup> coupled the recurrence plots with different measures, helpful for transforming graphical interpretations into statistical analysis. Many investigations were performed using such analysis.<sup>15–22</sup> Among the different measures used was the Shannon entropy which was found to be correlated with the inverse of the largest Lyapunov exponent. Since Shannon entropy characterizes distributions of statistical variables, it is not a dynamical invariant as the Kolmogorov entropy which characterizes properties of dynamical systems. A Shannon entropy is therefore not necessarily related to the largest Lyapunov exponent as the Kolmogorov entropy is according to the Pesin conjecture. Nevertheless, one of us recently proposed a new definition of the Shannon entropy, still computed from the recurrence plot, to obtain an entropy which increases when the chaotic dynamics is developed,<sup>23</sup> that is, which is related to the largest Lyapunov exponent.

The subsequent part of this paper is organized as follows: In Sec. II, it is briefly recalled how to properly compute the Shannon entropy from the recurrence plots. Section III describes the experimental device used for this study. Section IV, which is the main part of this paper, is devoted to the analysis of the dynamics underlying subject-ventilator system. Section V gives a conclusion.

## II. RECURRENCE PLOTS AND SHANNON ENTROPY

Before applying recurrence plots to investigate the dynamics underlying the subject-ventilator system, it is neces-

sary to discuss the conditions in which such an analysis can be safely performed. It has been shown that a recurrence plot analysis is optimal when the trajectory is embedded in a phase space reconstructed with an appropriate dimension  $d_E$ .<sup>24</sup> Such a dimension can be well estimated using a false nearest neighbor technique as introduced by Kennel *et al.*<sup>25</sup> or improved by Cao.<sup>26</sup> The  $d_E$ -dimensional phase space is thus reconstructed using delay coordinates. The time delay  $\tau$  can be estimated using mutual information<sup>27</sup> or the first zero of an autocorrelation function,<sup>28</sup> but most of the time a visual inspection works well too. Basically, the time delay has to be as small as possible and always less than a quarter of the pseudoperiod. A parameter specific to the recurrence plots is the threshold  $\epsilon$ . Many trials lead us to choose (for all the dynamics investigated) a threshold equal to  $\sqrt{d_E} \times 10\%$  of the average magnitude of the measured quantity. The threshold is therefore automatically computed from the time series investigated. Thus, only two parameters have to be determined: the embedding dimension,  $d_E$ , and the time delay,  $\tau$ . When not extracted from a Poincaré section, the time series used for computing recurrence plots and derived measures will be sampled at  $\tau$ . This appears to be a good balance between covering each oscillation and the whole attractor.

The Shannon entropy is usually defined as

$$S_{RP} = - \sum_{n=1}^H P_n \log(P_n). \quad (2)$$

In the form introduced by Trulla *et al.*,<sup>14</sup>  $H$  is the length of the maximum recurrent segment,  $P_n \neq 0$  is the relative frequency of the periodic segments with length  $n > 0$ . As well noted by Castellini and Romanelli, this “*quantity should be labeled more properly as a first rate cumulant since it is related to the relative frequency fluctuations.*”<sup>20</sup> In fact, since the Shannon entropy quantifies the complexity of the dynamics, it should increase when the chaotic behavior is developed, that is, for instance, when the bifurcation parameter  $\mu$  of the logistic map is increased. Moreover, according to the Pesin conjecture, the Shannon entropy must be correlated with the largest Lyapunov exponent.<sup>12</sup> Unfortunately, this is the opposite with the above definition.<sup>22</sup> Recently, one of us proposed to replace  $P_n$  with the relative frequency of the occurrence of the diagonal of segments with length  $n$  of non-recurrent points<sup>23</sup> and  $H$  is the maximum length of the non-recurrent segments. This definition removes the departure from the properties commonly presented by the Shannon entropy. In Sec. III, Shannon entropies will be computed from two different types of time series, namely the maxima of the airway pressure within a respiratory cycle and the times durations of these cycles. To avoid any confusion, the Shannon entropy will be designated by  $S_p$  when computed from the pressure and by  $S_T$  when computed from the time duration of the respiratory cycles.

This is simply justified since a white dot is represented by a nonrecurrent point which is nothing else than a signature of the complexity within the data. With this definition, the quantifier given by Eq. (2) increases as the bifurcation parameter increases (as shown in the case of the Logistic map in Fig. 1). As soon as the largest Lyapunov exponent is

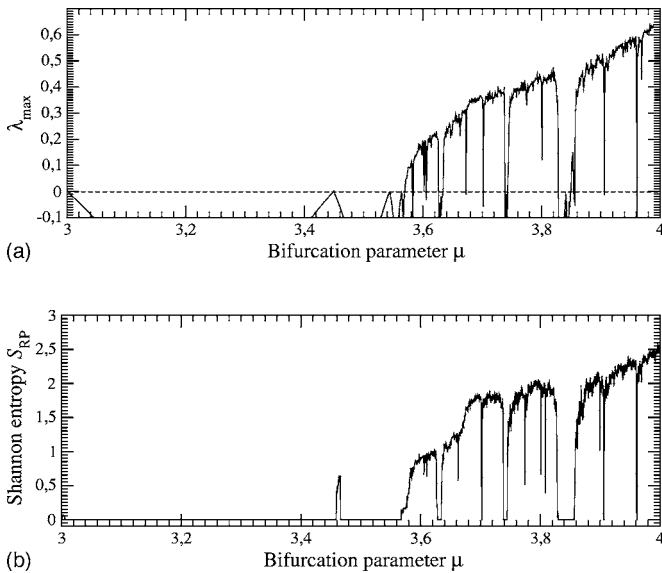


FIG. 1. Comparison between the largest Lyapunov exponent and the Shannon entropy for the Logistic function. (a) Largest Lyapunov exponent, (b) Shannon entropy  $S_{RP}$  computed from the recurrence plots. 1000 data points are here used.

positive, there is a one-to-one correspondence between the new definition of the quantifier  $S_{RP}$  and the largest Lyapunov exponent. In particular, when the dynamics is noise free, it is possible to identify periodic windows (at least the largest ones) as with the largest Lyapunov exponent (Fig. 1).

Recurrence plots can also be applied to continuous time series or to the set of intersections of the phase trajectory with the Poincaré section. The latter will be designated as a “discrete” time series. Indeed, we have to verify whether the dynamics is seen in the same way for both types of time series. The dependence of the Shannon entropy on a bifurcation parameter is thus computed from continuous time series solution to the Rössler system

$$\begin{aligned} \dot{x} &= -y - z, \\ \dot{y} &= x + ay, \\ \dot{z} &= b + z(x - c), \end{aligned} \tag{3}$$

with  $b=2$ ,  $c=4$ , and  $0.3 < a < 0.432$ , that is, over an interval where the bifurcation diagram is equivalent to those of the Logistic map. Consequently, a curve like those shown in Fig. 1(b) is expected. The Shannon entropy is successively computed from the time evolutions of the three dynamical variables of the Rössler system. The recurrence plots are computed by using a 3D phase space reconstructed with the delay coordinates. For each variable, the time delay  $\tau$  is equal to 1.5 s, that is, a quarter of the pseudoperiod of the Rössler system with the parameter range chosen. The data set is made of 1500 points sampled at  $\tau$ . For the three variables, the Shannon entropy is less sensitive to the dynamical change (Fig. 2). For instance, the period-3 window is not so clearly evidenced as in Fig. 1(b).

Moreover, there is a decrease of the entropy for  $a$  values greater than 0.425, a tendency not observed for the previous

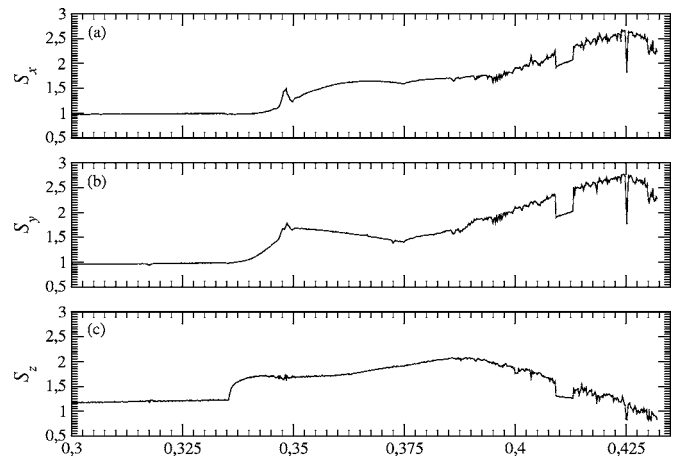


FIG. 2. Shannon entropy computed using recurrence plots from the different variables of the Rössler system. A 3D phase space is reconstructed using delay coordinates with a time delay  $\tau=1.5$  s. 1500 data points sampled at  $\tau$  are used.

computations in a Poincaré section [Fig. 1(b)]. On the other hand, the entropies computed from  $x$  and  $y$  are quite similar [Figs. 2(a) and 2(b)] but it decreases for  $a > 0.390$  when computed for the  $z$  variable [Fig. 1(c)]. This means that, when observed from the  $z$  variable, the underlying dynamics cannot be properly investigated. This dependence on the choice of the observable has been discussed in detail in Ref. 29. It therefore appears that investigating the dynamics using recurrence plots computed in a Poincaré section provides a more valuable characterization than when continuous time series are used. If possible, an analysis in the Poincaré section will be preferred.

### III. EXPERIMENTAL DEVICE AND MEASUREMENTS

#### A. The ventilatory circuit and the ventilator

The interplay between the patient and the ventilator is complex. Asynchronies may arise at several points during the respiratory cycle. In order to investigate this interplay, an experimental device is built as follows (Fig. 3). Noninvasive ventilation is delivered to the patient through a well-fitting full face mask (Mirage NV, RESMED, North Ride, Australia). To avoid  $\text{CO}_2$  rebreathing, an intentional leak is required in the ventilatory circuit and a Whisper Swivel II exhalation port (RESPIRONICS, Pittsburgh, PA) is therefore inserted (Fig. 3).

To adequately assist spontaneous breathing, a ventilator (Smartair ST, AIROX, Pau, France) is placed at the other end of the circuit. The ventilator detects inspiratory effort through changes in inspiratory flow. At the output of the ventilator, an antibacterial filter BB2000APS (PALL, Medical Newquay, UK) for breathing system is inserted to prevent bacterial contamination of the ventilator. In this study, the ventilator is used in a pressure support mode without backup frequency. The inspiratory phase is triggered by a threshold rate of airflow change, that is, by a variation of the flow  $\Delta_{20}=0.0167 \text{ l s}^{-1}$  over 20 ms. The ventilator thus delivers an inspiratory positive airway pressure (IPAP) which is set to several values between 10 and 20 mbar in the present proto-

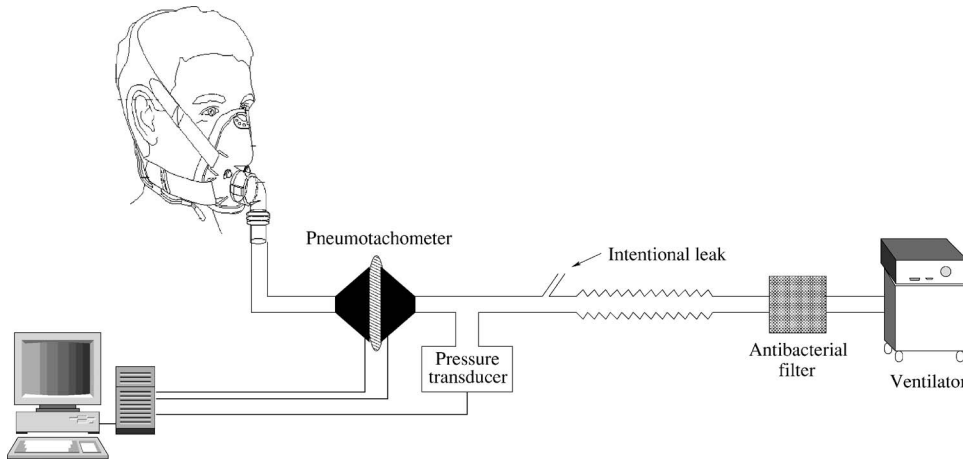


FIG. 3. Experimental device used for investigating the interplay between subject and ventilator. (See text for details.)

col. The pressure delivered by the ventilator then increases to the preset IPAP value during a so-called pressure risetime,  $T_{pr}$ . The expiratory phase is triggered here when the flow decreases below 75% of the maximal value of the peak flow. The pressure delivered by the ventilator then returns to the end positive airway pressure (EPAP) value which was set to 4 mbar in the present study. Few typical ventilatory cycles are depicted in Fig. 4.

During routine measurements of breathing pattern, respiratory flow ( $Q_v$ ) was measured using a pneumotachograph Fleisch #2 (METABO, Lausanne, Switzerland) connected to a pressure transducer TSD 160A ( $\pm 2.5$  cm H<sub>2</sub>O, BIOPAC SYSTEMS, Goletta, CA). The pneumotachograph was inserted between the full face mask and the exhalation port. Airway pressure ( $P_{aw}$ ) was measured with a differential pressure transducer DP15 ( $\pm 5.6$  cm H<sub>2</sub>O, VALIDYNE, Los Angeles, CA) near the pneumotachograph. All signals were digitalized at 100 Hz and sampled for analysis using an analogic/numeric acquisition system (MP150, BIOPAC SYSTEMS, Goletta, CA) running with a personal computer with the data acquisition software Acqknowledge ACK100.

**B. Subjects and protocol**

Twelve subjects (seven female and five male) with various health conditions were studied. All the subjects were in stable condition, as assessed by clinical examination and arterial blood gases. Among them, four patients had severe chronic obstructive pulmonary disease (COPD), four had obesity hypoventilation syndrome (OHS) and four were healthy subjects. The clinical characteristics of the 12 subjects are reported in Table I. The four COPD patients were smokers. The four OHS patients and the four healthy subjects were not. Basically, COPD is characterized by an increased airway resistance due to an inflammatory process in the bronchial wall and a loss of lung elastic recoil. Destruction of lung parenchyma causes loss of alveolar septa attachments and small airways obstruction can determine positive alveolar pressure at the end of expiration phase.<sup>30</sup> Therefore, airflow limitation leads to an intrinsic end positive airway pressure (EPAP<sub>i</sub>) and dynamic hyperinflation (i.e., increase of tele-expiratory volumes during excessive or high-

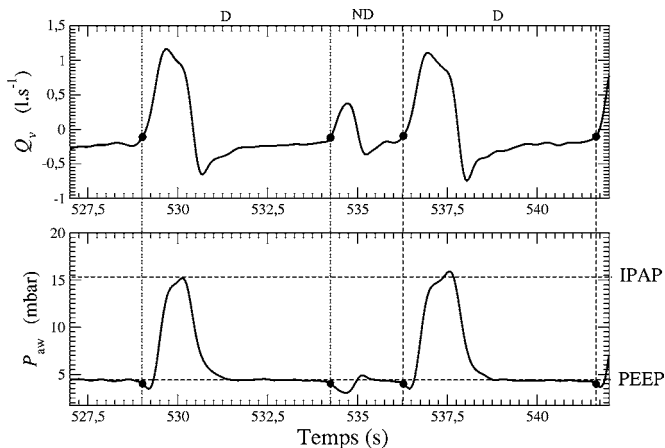


FIG. 4. Typical waveforms for the flow  $Q_v$  and the airway pressure  $P_{aw}$  during pressure support ventilation. Ventilator parameters: IPAP=16 mbar and EPAP=4 mbar. The second cycle is associated with an ineffective effort, that is, there is a small peak flow but without peak pressure.

TABLE I. Individual data for demographic, anthropometric, and functional characteristics of subjects in the study.<sup>a</sup>

Subject	Gender	Disease	BMI kg m <sup>-2</sup>	
1	F	COPD	22.2	Not familiar
2	M	COPD	21.4	Familiar
3	M	COPD	20.4	Not familiar
4	M	COPD	25.4	Familiar
5	F	OHS	55.7	Familiar
6	F	OHS	57.6	Familiar
7	F	OHS	48.0	Familiar
8	F	OHS	54.7	Not familiar
9	F	Healthy	23.1	Not familiar
10	F	Healthy	19.9	Not familiar
11	M	Healthy	24.8	Familiar
12	M	Healthy	25.5	Not familiar

<sup>a</sup>F=female, M=male. In the text, “patient” designates the subjects with diseases. The term “subject” will be used in a general way. COPD=chronic obstructive pulmonary disease and OHS =obstructive hypoventilation syndrome. BMI=body mass index.

frequency ventilation).<sup>31,32</sup> OHS is defined by the coexistence of obesity (body mass index greater than 30)<sup>34</sup> and daytime hypercapnia.<sup>33</sup> The mechanism of hypercapnia in OHS results from an alteration of ventilatory control (central component)<sup>35</sup> and/or a decreased thoraco-pulmonary compliance leading to a decreased work of breathing (peripheral component).<sup>36</sup>

Three of our patients ( $P_1$ ,  $P_3$ , and  $P_8$ ) and three healthy subjects ( $S_9$ ,  $S_{10}$ , and  $S_{12}$ ) were not familiar with noninvasive mechanical ventilation. The other five subjects were treated by noninvasive ventilation for at least three years and the healthy subject  $S_{11}$  was quite familiar with noninvasive ventilatory techniques. All subjects were informed about our study and their agreement was obtained before measurements.

The subjects were ventilated in a quiet seated position. Six working conditions were analyzed and compared in this study. The level of IPAP was increased from 10 to 20 mbar by 2 mbar steps. For each value, a 10-min period was recorded once a stable breathing pattern was observed. During the 10 min, great care was taken to avoid leaks.

#### IV. DYNAMICAL ANALYSIS

##### A. Phase portraits

Ideally, during mechanical ventilation the triggering of the ventilator should result from inspiratory muscles activity. The most frequent subject-ventilator asynchrony is when the subject's inspiratory effort does not trigger the ventilator.<sup>37,38</sup> Ineffective triggerings are very common in ventilator-dependent patients when dynamic hyperinflation is present, especially in COPD patients. In this situation, due to a high EPAP<sub>i</sub> and when pressure triggering is used, the patient cannot decrease the airway pressure below the EPAP<sub>i</sub> level and the inspiratory effort is therefore ineffective. Although ineffective triggering is commonly associated with COPD, it may also occur in patients with normal or restrictive lung disease, particularly when the preset IPAP value is high.

A cycle with patients' ineffective efforts corresponds to a lack of ventilator triggering. Despite this, there is still a peak flow (Fig. 4) that results from EPAP provided by the ventilator and the exhalation port which allows an input airflow. For all subjects studied here, inefficient efforts were always correlated to an oscillation of the airflow during the ventilatory cycle without peak pressure.<sup>39</sup> Thus, any significant muscular effort from the subject induces an airflow oscillation.

For instance, the healthy subject  $S_{12}$  had 41% of ineffective triggerings with an antibacterial filter but less than 3% when this filter was removed. Indeed, the filter can be viewed as a 64% increase of the threshold value  $\Delta_{20}Q_v$ .<sup>39</sup> From a clinical point of view, removing this filter can therefore be a solution to decrease the number of ineffective triggerings. The phase portraits reconstructed from the two time series of the airflow are shown in Fig. 5. When there is a large rate of ineffective triggering, the phase portrait is characterized by large loops associated with triggered cycles and small loops corresponding to nontriggered cycles [Fig. 5(a)]. When the rate of ineffective triggering is low (<3%), this

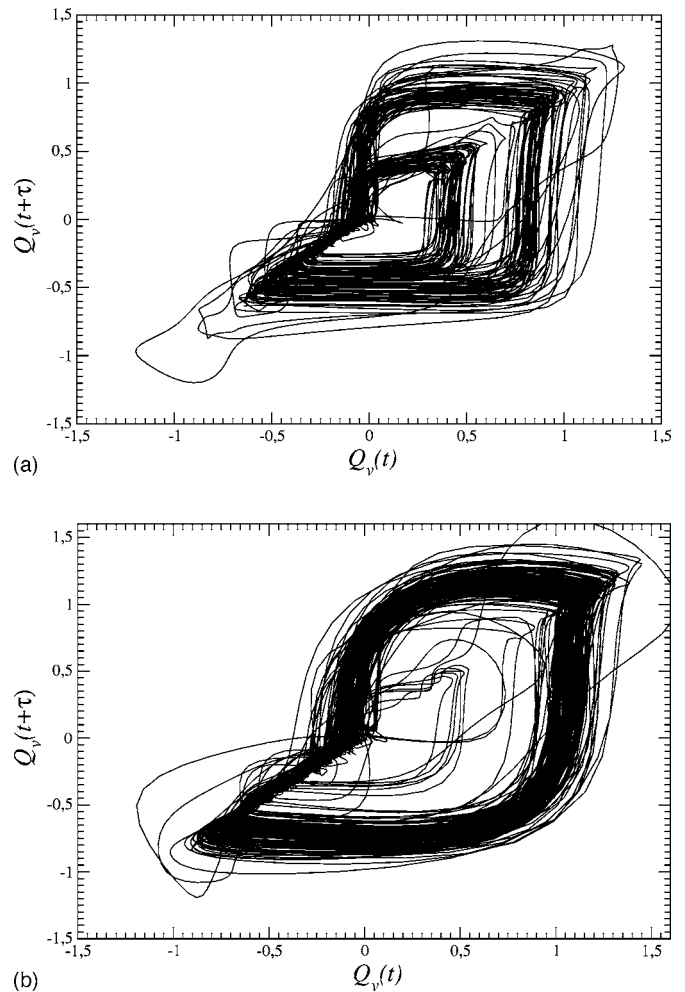


FIG. 5. Effect of an antibacterial filter placed in the ventilatory circuit on the occurrence of ineffective triggering. Phase portraits reconstructed from the airflow in subject  $S_{12}$  with IPAP=16 mbar. (a) With the filter: 41% of ineffective triggerings. (b) Without the filter: 3% of ineffective triggerings.

double structure is no longer observed and the phase portrait is mainly organized around a large loop [Fig. 5(b)]. Such a large loop can be viewed as a noisy limit cycle since a first-return map to a Poincaré section (not shown) has no other structure than those of a cloud of points. Such a lack of structure is the signature of a high-dimensional dynamics underlying the fluctuations around the limit cycle associated with the “ideal” ventilatory cycle. These fluctuations are thus considered as stochastic. They may result not only from swallows, coughings, etc., but also from some fluctuations produced by the central neural mechanism or the feedback loop of arterial chemoreceptors. The phase portrait can be traced during real-time monitoring and, consequently, it can be used by the physician to detect ineffective triggering in real time. In order to do that displaying the trajectory over a window of 5 min would be convenient.

##### B. Recurrence plot analysis

A plane projection of the phase portrait provides a global view of the ventilation. One of the advantages of the recurrence plots is that the succession of the events versus time can be followed. Since the recurrence plot analysis computed

in a Poincaré section helps to obtain a more reliable characterization (see Sec. II), the maximum of the airway pressure  $P_{\max}$  during a respiratory cycle is used to build a “discrete” time series. These maxima can be considered as equivalent to the set of the intersections of the phase trajectory with a Poincaré section. As an example, the recurrence plots are computed from the maxima of the airway pressure for subject  $S_{12}$  in working conditions similar to those of Fig. 5. The threshold  $\epsilon$  is set to  $\sqrt{d_E} \times 0.1 \times \text{IPAP}$ . Compared to the phase portraits, we now have a representation of the succession of the cycles, black domains corresponding to recurrences of the dynamics, that is, succession of similar cycles (Fig. 6). Since the rate of ineffective efforts is always less than 50%, one can expect that a recurrence plot with a large number of black domains will correspond to a mechanical ventilation with a low rate of asynchronisms.

This is checked by the recurrence plots shown in Fig. 6. The recurrent points are quite rare when the antibacterial filter is inserted [Fig. 6(a)]. This means that consecutive cycles are very different from the pressure point of view, that is, a triggered cycle is very often followed (or preceded) by a nontriggered cycle and vice versa. As soon as the filter is removed [Fig. 6(b)], the nontriggered cycles decrease to 3% and the recurrence plot is almost black everywhere. Only small sets of cycles reveal large fluctuations of the airway pressure, that is, asynchronisms. From the recurrence plots, it can therefore easily deduced that the mechanical ventilation is much more efficient when the antibacterial filter is removed.

The Shannon entropy is computed from these recurrence plots according to our new definition. When computed from the recurrence plots built from the maxima of the airway pressure, the Shannon entropy will be denoted as  $S_p$ . It is equal to 2.3 with the filter and equal to 0.4 with the filter. As expected, when the ineffective efforts are not frequent, the Shannon entropy is significantly smaller than when inefficient efforts are numerous. The Shannon entropy  $S_p$  is computed for the 69 data sets recorded in our protocol. It is strongly correlated to the rate of asynchronisms (nontriggered cycles) (Fig. 7). The Shannon entropy  $S_p$  is therefore a good quantifier of the rate of asynchronisms. In a previous study,<sup>39</sup> we found that an asynchronism frequency below 10% was not relevant for ventilatory comfort. This 10% corresponds to a Shannon entropy that is slightly less than 1. Thus, according to this previous study, a Shannon entropy  $S_p$  less than 1 corresponds to a situation where inefficient efforts are not clinically relevant to the subjects’ comfort.

Another dynamical characteristic relevant for the quality of the assisted mechanical ventilation is the rate of fluctuations of the total duration of the respiratory cycle. Since the subject is in a quiet seated position, there is no particular muscular activity which could affect the oxygen blood rate. Thus, at least for healthy subjects, the breathing rhythms should be regular. In particular, the patients very familiar with mechanical ventilation should be able to manage their ventilator for breathing in a regular way. Indeed, we assume that the more regular the dynamics, the better the comfort. It is therefore important to investigate the fluctuations over the total duration of the respiratory cycle,  $T_{\text{tot}}$ . As we will see,

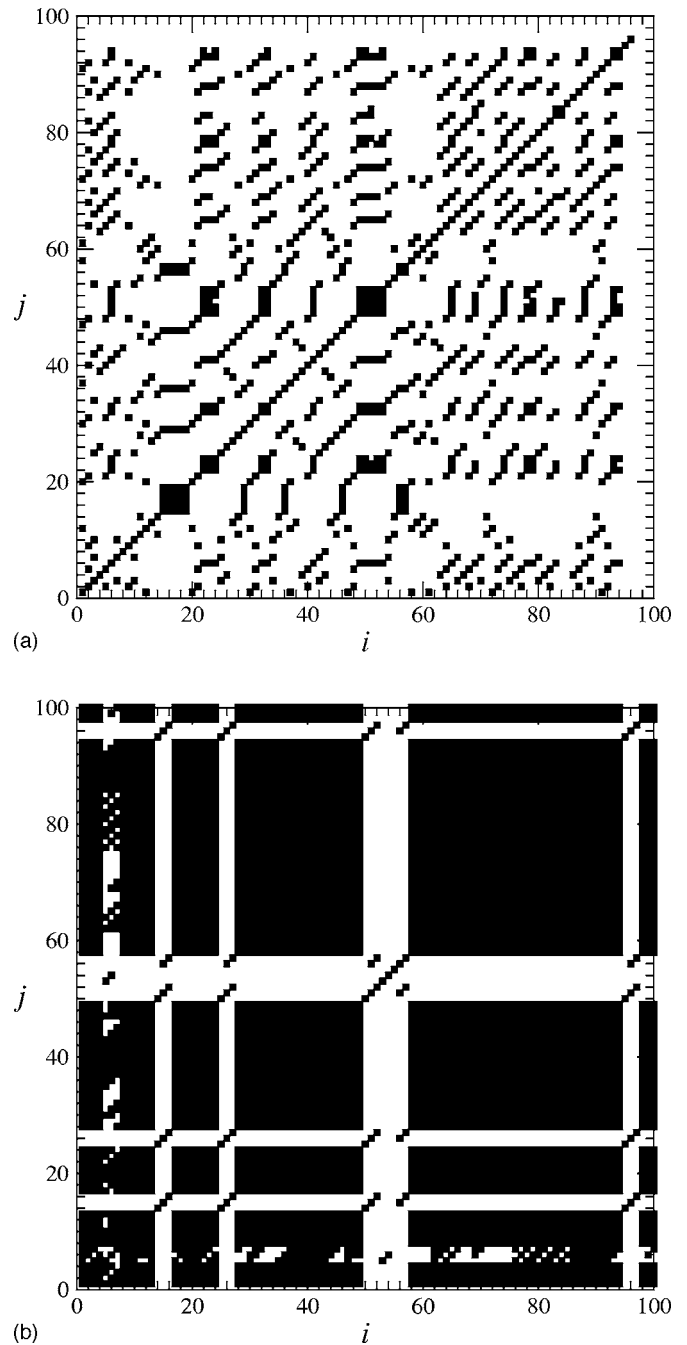


FIG. 6. Recurrence plots computed from the maxima of the pressure airway during respiratory cycles recorded for subject  $S_{12}$  with and without an antibacterial filter. (a) With the filter: 41% of ineffective triggerings. (b) Without the filter: 3% of ineffective triggerings.

such fluctuations are not necessarily correlated with the occurrence of asynchronisms. Such a lack of correlation invites us to treat this problem as a bivariate time series problem by using cross recurrence plots as introduced in Ref. 40, but this is out of the scope of the present paper and is postponed for future works.

Recurrence plots are therefore computed from  $T_{\text{tot}}$  using a threshold  $\epsilon$  set to  $\sqrt{d_E} \times 0.1 \times \bar{T}$ , where  $\bar{T}$  is the “ideal” time duration cycle corresponding to a respiratory frequency equal to 12 breaths per min. For the two cases investigated in Figs. 5 and 6, the recurrence plots also reveal obvious depar-

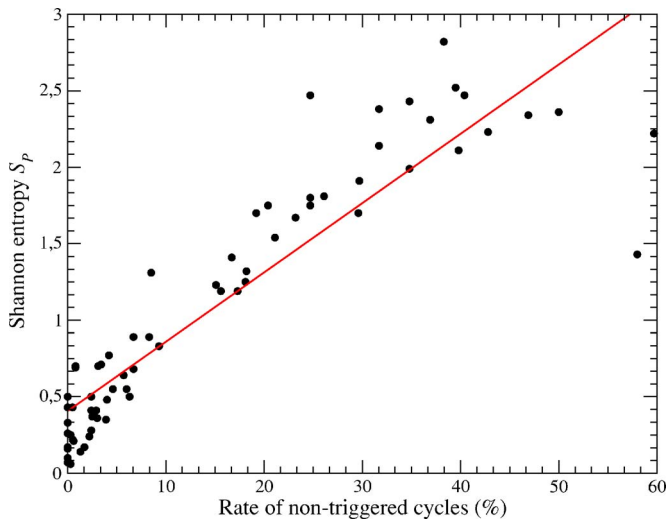
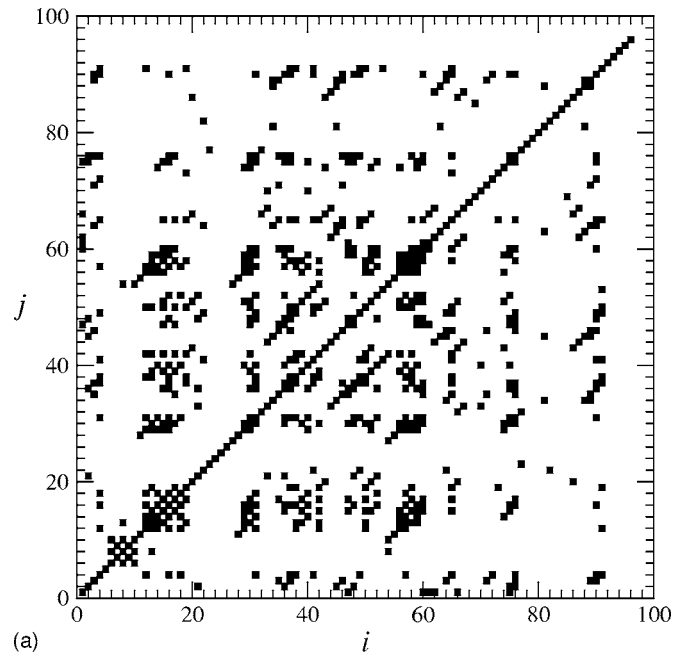


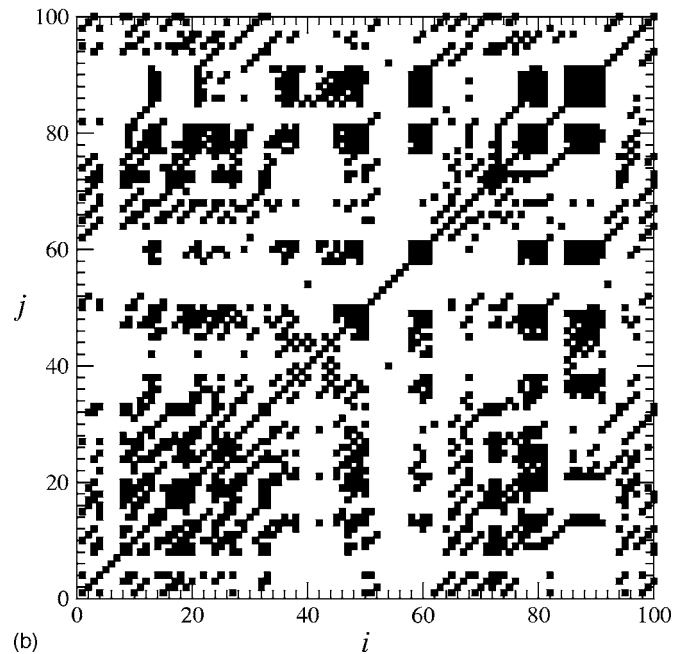
FIG. 7. (Color online) Dependence of the Shannon entropy on the rate of asynchronisms. A positive correlation is clearly evidenced by a linear regression.

tures but not in the same way as when computed from  $P_{\max}$ . With the filter, both recurrence plots, from  $P_{\max}$  [Fig. 6(a)] and  $T_{\text{tot}}$  [Fig. 8(a)], are quite similar as revealed by the Shannon entropy,  $S_p=2.3$  and those computed from  $T_{\text{tot}}$ ,  $S_T=2.5$ . The fact that  $S_T$  is slightly greater than  $S_p$  means that the lack of recurrences over  $T_{\text{tot}}$  affects a slightly larger number of cycles than those over  $P_{\max}$ . Two reasons may be invoked: (i) The asynchronisms affect not only the nontriggered cycles but also some of the following ones and (ii) there is another origin from the fluctuations over the total duration of the respiratory cycles than the ability to trigger the ventilator. The first reason seems to be natural but the second one cannot be rejected too, as shown by the recurrence plot computed from  $T_{\text{tot}}$  with the filter [compare Fig. 6(b) with Fig. 8(b)]. The regularity of the breathing rhythm is thus not only correlated with the occurrence of asynchronisms. This is obviously confirmed by the Shannon entropy, since  $S_T=1.9 \gg S_p=0.4$  for subject  $S_{12}$  without the filter. There is therefore some other origins for not having a regular breathing rhythm. These origins are not necessarily associated with a pathology since subject  $S_{12}$  is healthy. Note that subject  $S_{12}$  was not familiar with mechanical ventilation.

The Shannon entropy  $S_T$  was computed for the 69 data sets recorded and plotted versus the Shannon entropy  $S_p$  (Fig. 9). Basically, four different regions are distinguished in this figure. First, the square defined by  $S_T < 1$  and  $S_p < 1$  corresponds to subjects who have fluctuations neither over  $P_{\max}$ , nor over  $T_{\text{tot}}$ . There is no ambiguity for these subjects since they have almost no asynchronism and their breathing rhythms are very regular. Only three subjects,  $S_4$ ,  $S_7$ , and  $S_{11}$ , have two Shannon entropies less than 1 for most of the IPAP values. These three subjects were familiar with noninvasive mechanical ventilation. Note that one has a COPD, one has an OHS, and one is a healthy subject. The ability to manage the ventilator is therefore not linked to pulmonary pathology. One may expect that these subjects are comfortable under their ventilator.



(a)



(b)

FIG. 8. Recurrence plots computed from the total duration of the cycle,  $T_{\text{tot}}$ , recorded for subject  $S_{12}$  with and without an antibacterial filter in the ventilatory circuit. (a) With the filter: 41% of ineffective triggerings. (b) Without the filter: 3% of ineffective triggerings.

Second, there is the rectangle defined by  $S_T > 1$  and  $S_p < 1$ . These data sets correspond to subjects with less than 10% of nontriggered cycles but quite significant fluctuations over the total duration of the ventilatory cycle. They correspond to the case investigated in Figs. 5(b), 6(b), and 8(b). COPD patient  $S_1$  is under these conditions for all the IPAP values and subject  $S_9$  for most of them. Both were not familiar with noninvasive mechanical ventilation. COPD patient  $S_2$  is also under these conditions for low IPAP values (IPAP less than 16 mbar). There is no OHS patient under these conditions. This feature suggests that, in general, OHS pa-

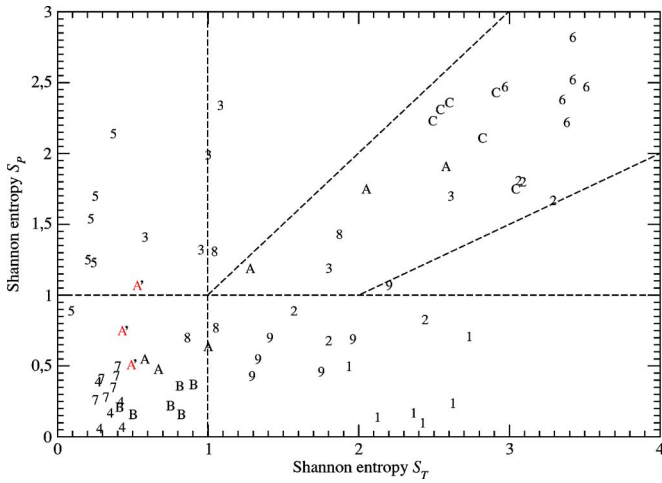


FIG. 9. (Color online) Shannon entropy  $S_T$  versus Shannon entropy  $S_p$  for the 69 data sets recorded during our protocol. Integers  $i (i \in [1; 9])$  designate subjects  $S_i$  for the six measurements at different IPAP values. Letters A, B, and C designate subjects  $S_{10}$ ,  $S_{11}$ , and  $S_{12}$ , respectively.

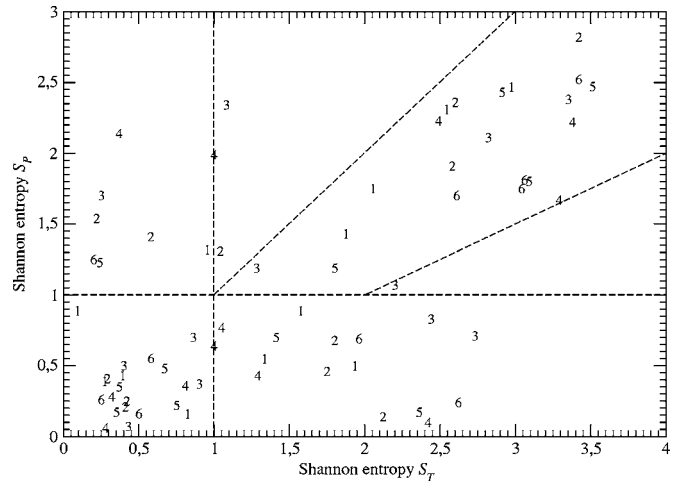


FIG. 10. Shannon entropy  $S_T$  versus Shannon entropy  $S_p$  for the 69 data sets recorded during this study. Integers  $i$  correspond to the  $i$ th IPAP value according to 10, 12, 14, 16, 18, and 20, respectively.

tients would not display significant fluctuations over the total duration of the ventilatory cycle,  $T_{tot}$ . Obesity tends to reduce lung volumes and there is no longer possibility for varying the inspiratory volume and, consequently, for varying the time duration of the respiratory cycle, at least when there is no asynchronism. The subjects who are under these conditions ( $S_T > 1$  and  $S_p < 1$ ) are therefore not familiar with non-invasive mechanical ventilation and would be able to induce fluctuations of their breathing rhythm, mainly by increasing the work of breathing in order to trigger the ventilator.

Third, the rectangle is defined by  $S_T < 1$  and  $S_p > 1$ . For these cases, there are many ineffective efforts although the breathing rhythm is regular. Two patients correspond to these conditions, one COPD and one OHS. The COPD patient  $S_3$  was not familiar with mechanical ventilation. Nevertheless, he was very careful about his breathing (nothing particular was asked of him) and he was thus able to keep his respiratory rhythm constant, although it was unpleasant for him. Indeed, he was tired at the end of the six measurement periods. OHS patient  $S_5$  was familiar with mechanical ventilation. This patient was therefore able to keep constant the time duration of his respiratory cycles although numerous cycles were not triggered. We believe that these patients were able to “manage” their ventilator by imposing a constant total duration for the respiratory cycle, in spite of many asynchronisms. Their pathology prevents them from a great ability to trigger the ventilator but their ventilatory command and their respiratory muscles can provide the work of breathing, whatever the asynchronism rate.

The fourth part of the graph shown in Fig. 9 is associated with a sector such as  $S_T > 1$  and  $S_p > 1$ . But all the points obeying to such conditions are not spread over this whole upper right rectangle but are mainly in a restricted sector between the first bisecting line (defined by  $S_p = S_T$ ) and another line defined by  $S_p = 0.5S_T$ . Both are displayed in Fig. 9 as diagonal dashed lines. The fact that all the points are located below the bisecting line means that, in general,  $S_p < S_T$ , with the exception of the third case previously men-

tioned. This results from the fact that a nontriggered cycle has some effects on the preceding and the following cycles. The fluctuations over the time duration affects thus more numerous cycles than fluctuations over  $P_{max}$ . Most of the points located in this fourth sector correspond to subjects not familiar with a mechanical ventilation (only patient  $S_2$  and  $S_6$  are familiar). For all of these subjects, being not familiar with mechanical ventilation there is an obvious correlation between  $S_p$  and  $S_T$  (with a coefficient of correlation of about 1). For these patients, the fluctuations over the time duration  $T_{tot}$  results from the asynchronisms. We conjecture that, for most of them, they can be trained. For instance, the healthy subject  $S_{10}$  presented  $S_T > 1$  and  $S_p > 1$  for IPAP values smaller than 16 mbar. In fact, it was the three first periods of 10 min during which this subject was assisted by noninvasive mechanical ventilation. A few months later, these three data sets were recorded again with the same subject. For all of them, the rate of nontriggered cycles decreased below 10% and both entropies became smaller than 1 (points marked by  $A'$  in Fig. 9). Unfortunately, we were not able to repeat the measurements with the other patients who were not familiar with mechanical ventilation. There are also some subjects who had one or two points located in the fourth sector: this will mainly depends on the parameter settings of the ventilator as the IPAP value. Patient-ventilator interactions characterized by a point in this fourth section do not correspond to the best conditions for assisted mechanical ventilation and we can expect that the quality of their ventilation, at least from the mechanical point of view, could be improved by changing the parameter setting of the ventilator or by training the patient.

These investigations lead us to four classes as follows:

- (1)  $S_p < 1$  and  $S_T < 1$  familiar;
- (2)  $S_p < 1$  and  $S_T > 1$  not familiar, COPD or healthy;
- (3)  $S_p > 1$  and  $S_T < 1$  familiar or careful about its breathing rhythm, inefficient efforts;
- (4)  $S_p > 1$  and  $S_T > 1$  not familiar or not optimize the parameter setting, inefficient efforts.

By plotting the Shannon entropy  $S_P$  versus the Shannon entropy  $S_T$  according to the IPAP value set for the measurements (independently of the subject under considerations), it occurs that there is no relationship between each of the sectors of the graph and the IPAP value (Fig. 10). Indeed, any IPAP value is found in each sector. The IPAP value is therefore a not so relevant parameter for the variability in the dynamics underlying patient-ventilator interactions.

## V. CONCLUSION

Recurrence plots can be used to investigate the properties of complex dynamics as widely used, particularly in biomedicine. A new definition for the Shannon entropy has been proposed to obtain an entropy which increases as the chaotic dynamics is more developed as expected for a Shannon entropy. In particular, we showed that it is now strongly correlated to the largest Lyapunov exponent, according to Pesin's conjecture. Although Shannon entropies are not necessarily dynamical invariants, the Shannon entropy computed in a Poincaré section is related to the largest Lyapunov exponent which is a dynamical invariant. Thus, the Shannon entropy computed from the maxima of the airway pressure—or any other dynamical variable—is also a dynamical invariant as Renyi entropy which can also be estimated from recurrence plots.<sup>41</sup> Note that the Shannon entropy computed from the time duration of cycles can be safely considered as a dynamical invariant only in the case of phase coherent dynamics. It remains an open questions in other cases.

The recurrence plots and the associated Shannon entropy were used to investigate the dynamics underlying patient-ventilator interactions. In particular, we were able to show that, at least two dynamical measures are useful to characterize the quality of the noninvasive mechanical ventilation, namely the Shannon entropies computed from the maxima of the airway pressure and from the total duration of the ventilatory cycle. The first entropy estimates the rate of asynchronisms (ineffective triggerings) and the second entropy quantifies the fluctuations over the total duration of ventilatory cycles. These two measures are not necessarily correlated and strongly depends whether the subjects are familiar to mechanical ventilation or not. Basically, when these two entropies are less than 1, it can be assumed that, from a mechanical point of view, the parameter setting of the ventilator are optimal. Chest physicians may use these quantifiers computed in real time to optimize the settings of the ventilators. It is clear that learning to breathe under the influence of a ventilator is a significant factor determining the entropy of the resulting signal. Thus, these quantifiers can be used to determine the quality of the patient-ventilator interactions but cannot be used to make a diagnostic statement, at least until patients with similar experience with the respirator are considered.

## ACKNOWLEDGMENTS

C.L. wishes to thank Wassila Hamadene and Laurent Peyrodie for stimulating discussions about recurrence plots analysis. We thank Brigitte Fauroux (Trousseau Hospital, Paris) for her stimulating encouragements.

- <sup>1</sup>G. A. Petrillo, L. Glass, and T. Trippenbach, "Phase locking of the respiratory rhythm in cats to a mechanical ventilator," *Can. J. Physiol. Pharmacol.* **61**, 599–607 (1983).
- <sup>2</sup>G. A. Petrillo and L. Glass, "A theory for phase locking respiration in cats to a mechanical ventilator," *Am. J. Physiol.* **246**, R311–R320 (1984).
- <sup>3</sup>A. L. Goldberger and B. J. West, "Applications of nonlinear dynamics to clinical cardiology," *Ann. N.Y. Acad. Sci.* **504**, 155–212 (1987).
- <sup>4</sup>A. Babylogantz and A. Destesche, "Is the normal heart a periodic oscillator?" *Biol. Cybern.* **58**, 203–211 (1988).
- <sup>5</sup>J. Kurths, A. Voss, P. Saparin, A. Witt, H. J. Kleiner, and N. Wessel, "Quantitative analysis of heart rate variability," *Chaos* **5**, 88–94 (1995).
- <sup>6</sup>M. E. D. Gomes, A. V. P. Souza, H. N. Guimaraes, and L. A. Aguirre, "Investigation of determinism in heart rate variability," *Chaos* **10**, 398–410 (2000).
- <sup>7</sup>L. A. Aguirre, V. C. Barros, and A. V. P. Souza, "Nonlinear multivariate modeling and analysis of sleep apnea time series," *Comput. Biol. Med.* **29**, 207–228 (1999).
- <sup>8</sup>E. N. Bruce and J. A. Daubenspeck, "Mechanisms and analysis of ventilatory stability," in *Regulation of Breathing*, edited by J. A. Dempsey and A. I. Pack (Dekker, New York, 1995), pp. 285–313.
- <sup>9</sup>T. Brack, A. Jubran, and M. J. Tobin, "Dyspnea and decreased variability of breathing in patients with restrictive lung disease," *Am. J. Respir. Crit. Care Med.* **165**, 1260–1264 (2002).
- <sup>10</sup>B. Loveridge, P. West, N. R. Anthonisen, and M. H. Kryger, "Breathing patterns in patients with chronic obstructive pulmonary disease," *Am. Rev. Respir. Dis.* **130**, 730–733 (1984).
- <sup>11</sup>V. L. Schechtman, M. Y. Lee, A. J. Wilson, and R. M. Harper, "Dynamics of respiratory patterning in normal infants and infants who subsequently died of the sudden infant death syndrome," *Pediatr. Res.* **40**, 571–577 (1996).
- <sup>12</sup>Ya B. Pesin, *Dimension Theory in Dynamical Systems* (University of Chicago Press, Chicago, 1998).
- <sup>13</sup>J.-P. Eckmann, S. Oliffson Kamphorst, and D. Ruelle, "Recurrence plots of dynamical systems," *Europhys. Lett.* **4**, 973–977 (1987).
- <sup>14</sup>L. L. Trulla, A. Giuliani, J. P. Zbilut, and C. L. Webber, Jr., "Recurrence quantification analysis of the logistic equation with transients," *Phys. Lett. A* **223**, 255–260 (1996).
- <sup>15</sup>J. P. Zbilut, M. Koebe, H. Loeb, and G. Mayer-Kress, "Use of recurrence plots in the analysis of heart beat intervals," in *Proceedings of the IEEE Conference on Computers in Cardiology* (IEEE Computer Society, Chicago, 1991), pp. 263–266.
- <sup>16</sup>P. Faure and H. Korn, "A new method to estimate the Kolmogorov entropy from recurrence plots: its application to neuronal signals," *Physica D* **122**, 265–279 (1998).
- <sup>17</sup>J. P. Zbilut, C. L. Webber, Jr., A. Colosimo, and A. Giuliani, "The role of hydrophobicity patterns in prion folding as revealed by recurrence quantification analysis of primary structure," *Protein Eng.* **13**, 99–104 (2000).
- <sup>18</sup>J. Belaire-Franch, D. Contreras, and L. Tordera-Lledó, "Assessing nonlinear structures in real exchange rates using recurrence plot strategies," *Physica D* **171**, 249–264 (2002).
- <sup>19</sup>P. Babinec, L. Zemanová, and M. Babincová, "Randomness and determinism in human heart-beat dynamics: Recurrence plot analysis," *Phys. Medica* **18**, 63–67 (2002).
- <sup>20</sup>H. Castellini and L. Romanelli, "Applications of recurrence quantified analysis to study the dynamics of chaotic chemical reaction," *Physica A* **342**, 301–307 (2004).
- <sup>21</sup>L. Parrott, "Analysis of simulated long-term ecosystem dynamics using visual recurrence analysis," *Ecol. Complexity* **1**, 111–125 (2004).
- <sup>22</sup>W. Hamadene, "Systèmes chaotiques et méthode des récurrences: application à la détection précoce des crises d'épilepsie," Ph.D. thesis, University of Lille (2005).
- <sup>23</sup>C. Letellier, "Estimating the Shannon entropy: recurrence plots versus symbolic dynamics," *Phys. Rev. Lett.* **96**, 254102 (2006).
- <sup>24</sup>J. P. Zbilut and C. L. Webber, Jr., "Embeddings and delays as derived from quantification of recurrence plots," *Phys. Lett. A* **171**, 199–203 (1992).
- <sup>25</sup>M. B. Kennel, R. Brown, and H. D. I. Abarbanel, "Determining embedding dimension for phase-space reconstruction using a geometrical construction," *Phys. Rev. A* **45**, 3403–3411 (1992).
- <sup>26</sup>L. Cao, "Practical method for determining the minimum embedding dimension of a scalar time series," *Physica D* **110**, 43–52 (1997).
- <sup>27</sup>A. M. Fraser and H. L. Swinney, "Independent coordinates for strange attractors from mutual information," *Phys. Rev. A* **33**, 1134–1140 (1986).
- <sup>28</sup>W. Liebert and H. G. Schuster, "Proper choice of the time delays for the analysis of chaotic time series," *Phys. Lett. A* **142**, 107–111 (1989).
- <sup>29</sup>C. Letellier and L. A. Aguirre, "Investigating nonlinear dynamics from

- time series: the influence of symmetries and the choice of observables," *Chaos* **12**, 549–558 (2002).
- <sup>30</sup>A. Rossi, G. Polese, G. Blandi, and G. Conti, "Measurement of static compliance of total respiratory system in patients with acute respiratory failure during mechanical ventilation," *Intensive Care Med.* **21**, 522–536 (1995).
- <sup>31</sup>P. E. Pepe and J. J. Marini, "Occult positive end expiratory pressure mechanically ventilated patients with airflow obstruction, the auto-PEEP effect," *Am. Rev. Respir. Dis.* **126**, 160–170 (1982).
- <sup>32</sup>A. Rossi, S. B. Gottfried, L. Zocchi, B. D. Higgs, S. Lennox, P. M. A. Calverley, P. Begin, A. Grassino, and J. Milic-Emili, "Measurement of static compliance of total respiratory system in patients with acute respiratory failure during mechanical ventilation," *Am. Rev. Respir. Dis.* **131**, 672–677 (1985).
- <sup>33</sup>J. F. Masa, B. R. Celli, J. A. Riesco, M. Hernandez, J. Sanchez de Cos, and C. Disdier, "The obesity hypoventilation syndrome can be treated with noninvasive mechanical ventilation," *Chest* **119**, 1102–1107 (2001).
- <sup>34</sup>J.-F. Muir, A. Cuvelier, S. Bota, F. Portier, D. Benhamou, and G. Onea, "Modalities of ventilation in obesity," *Monaldi Arch. Chest Dis.* **53**, 556–559 (1998).
- <sup>35</sup>S. Krachman and G. J. Criner, "Hypoventilation syndromes," *Clin. Chest Med.* **19**, 139–155 (1998).
- <sup>36</sup>J. T. Sharp, J. P. Henry, S. K. Sweany, W. R. Meadows, and R. J. Pietraszt, "The total work of breathing in normal and obese men," *J. Clin. Invest.* **43**, 728–739 (1964).
- <sup>37</sup>D. Georgopoulos, M. Anastasaki, and K. Katsanoulos, "Effects of mechanical ventilation on control breathing," *Monaldi Arch. Chest Dis.* **52**, 253–262 (1997).
- <sup>38</sup>M. J. Tobin, K. L. Young, and F. Laghi, "Patient-ventilator interaction," *Am. J. Respir. Crit. Care Med.* **163**, 1059–1063 (2001).
- <sup>39</sup>L. Achour, C. Letellier, A. Cuvelier, E. Vérin, and J.-F. Muir, "Asynchrony and cyclic variability in pressure support noninvasive ventilation," *Comput. Biol. Med.* (in press).
- <sup>40</sup>M. C. Romano, M. Thiel, J. Kurths, I. Z. Kiss, and J. L. Hudson, "Detection of synchronization for non-phase-coherent and non-stationary data," *Europhys. Lett.* **71**, 466–472 (2005).
- <sup>41</sup>M. Thiel, M. C. Romano, P. L. Read, and J. Kurths, "Estimation of dynamical invariants without embedding by recurrence plots," *Chaos* **14**, 234–243 (2004).